the control operation is within the operating limit of the machine, then control operation is allowed to take place, else it is aborted.

The hardware and software of this system has been developed and installed. The view of MOVPE machine is shown in Fig.L.6.2. The system is presently being operated on trial basis. Software for automation of growth process with sequential programming feature and recipe is to be implemented soon.

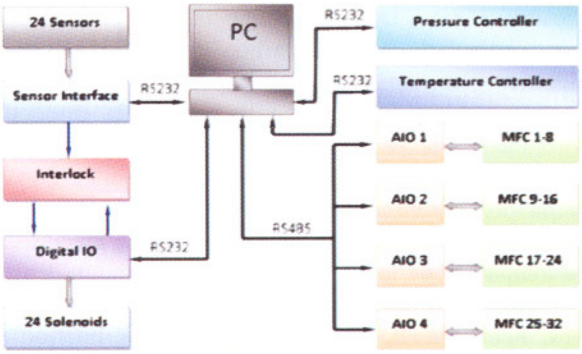

Fig. L.6.1 : A schematic of the control system.

Fig. L.6.2: A view of MOVPE system with the AIO control units in operation

Reported by:
V. P. Bhanage (viraj@rrcat.gov.in),
T. Ganguli, and C. P. Navathe

L.7: Multi-keV x-ray dispersionless spectrograph based on the x-ray CCD camera

A multi-keV x-ray spectrograph based upon back illuminated x-ray CCD detector has been set up and characterized in the Laser Plasma Division of RRCAT. This spectrograph covers a spectral range of 2 - 20 keV and has a spectral resolution better than ~3 %. It has been used to measure the x-ray continuum and K- α line emission from femtosecond laser irradiated targets.

The study of K-α radiation produced by interaction of ultra-short, ultra-intense laser pulses has been a subject of considerable importance for research investigations of inertial confinement fusion and potential application in femtosecond x-ray probing. Such x-rays originate from the fast electrons generated by the laser interaction with the target surface. They penetrate into the cold target material to generate continuum hard x-ray bremsstrahlung and characteristic K- α line radiation.

The underlying principle of a dispersionless spectrograph is operation of a solid state detector (such as Si(Li), Ge(Li)) in "single photon counting" mode. The incident x-ray photon converts into electron-hole pairs whose number is proportional to the incident photon energy. The photon energy is stored into the energy channels of a multi-channel analyser and the spectrum is built over several events. However, such a system tends to be bulky, costly, and needs data to be collected over several thousands of shots. In order to make the spectrograph compact and single-shot, an x-ray CCD camera has been used as the detector. In this case, the spectrum is simply a histogram of the energy of the x-ray photons received by the various pixels of the CCD. Thus, it enables one to record the spectrum without any dispersive element. Back-side illuminated, thinned CCD cameras are preferred to extend the detection range to high x-ray energies.

The high energy x-ray spectrograph has been set up and characterized for recording x-ray spectrum from plasma produced by 45 fs Ti:sapphire laser focussed to an intensity $\sim 10^{18}$ W-cm^{-2}. The spectrograph consists of an x-ray CCD camera (Reflex SRO, Model: X-Vision 4M) equipped with a back-illuminated chip (E2V) consisting of 2048 x 2048 pixels, each of 13.5 x 13.5 μm^2 size. The CCD chip has a regulated two-stage thermo-electric cooler to cool the CCD chip down to -30° C to reduce the thermal noise. The CCD output is digitalized by a 16 bit ADC. The readout noise is < 7 counts (rms) at 30° C. The detector is kept at a distance of 580 mm with a collimator subtending a solid angle of ~ 9.3 x 10^{-4} steradian. Appropriate filters (depending on target material) are used to attenuate the signal to operate in single photon counting mode (i.e. not more than one photon falls on each pixel every shot). The data was analysed with the versatile image processing software *"Promise"* developed by the Laser Systems Engineering Division of RRCAT.

The spectrograph was used to record the x-ray spectrum of laser produced plasma of various targets such as Ti, Cu, Zn, Ga, As, Zr, and Mo. Fig.L.7.1 shows the x-ray spectrum of titanium. The K-α (4.5 keV) and K-β (4.9 keV) lines, along with continuum emission, can be clearly seen. It also shows the spectrum of stainless steel (SS). The K-α lines of Cr (5.4 keV), Fe (6.4 keV) and Ni (7.5 keV) (constituents of SS) can be seen.

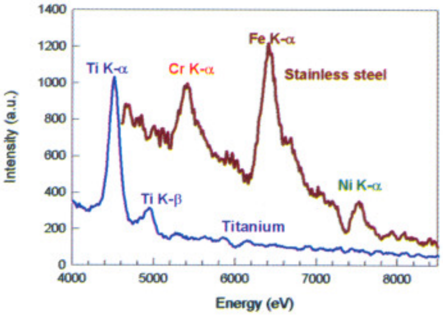

Fig. L.7.1: X-ray spectrum of Ti and stainless steel in the energy range around the inner shell transitions.

Under the same experimental conditions, the FWHM of the histogram of a dark frame was ~ 10 counts, resulting in a lower limit on the energy resolution of the spectrograph as ~ 67 eV. The energy resolution from the ionization statistics is ~ 109 eV. Thus, the overall resolution is expected to be ~ 128 eV. The FWHM of the Ti K-α line radiation (Fig.L.6.1) is measured to be ~ 136 eV, which is in close agreement with the theoretically expected resolution. Fig.L.7.2 shows the plot of photon energy as a function of CCD count. The plot shows a linear response with the photon energy in the whole spectral range. The X-intercept is due to the noise which gives a background count of ~ 270. The slope gives a calibration factor of ~ 6.78 [i.e.: Energy = 6.78 * (Counts - 270) eV] .The upper and lower limits on the spectral range of detection come from the CCD depletion region depth and the background counts respectively.

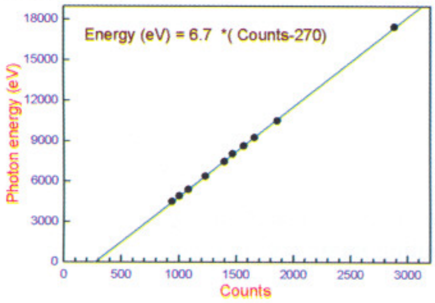

Fig. L.7.2: Calibration of the spectrograph in the 4 - 18 keV spectral range.

Reported by :
V.Arora (arora@rrcat.gov.in) and P.A.Naik

L.8: Pre-welding laser surface treatment to enhance inter-granular corrosion resistance of gas tungsten arc weldment of type 304 stainless steel

A novel pre-welding laser surface treatment has been developed by Laser Material Processing Division of RRCAT for gas tungsten arc welding (GTAW) of austenitic stainless steel, to effectively enhance its resistance against heat-affected zone (HAZ) sensitization and inter-granular corrosion (IGC). During welding of austenitic stainless steels, particularly of high carbon content, HAZ of the weldment gets sensitized, which adversely affects its resistance against IGC during its service in susceptible environment. The phenomenon is referred as "weld decay". IGC of austenitic stainless steel arises from inter-granular precipitation of chromium-rich carbides in the temperature range of 773 - 1073 K. Inter-granular carbide precipitation is accompanied by the development of chromium-depleted zone adjacent to grain boundaries. Chromium-depleted zones, being anodic with respect to grain interior, are preferentially attacked in the corrosive environment leading to IGC. This state is referred as "sensitization". IGC is one of the major problems experienced by welded components of austenitic stainless steel, operating in process industry.

The present study was performed on 6 mm thick medium carbon (0.044 wt %) and 10 mm thick high carbon (0.1 wt %) sheets of type 304 stainless steel. Laser surface treatment was performed with an indigenously developed 4 kW CO_2 laser operated in pulse-periodic mode. The results of the experimental study established that surface modification induced by pre-weld CO_2 laser treatment is highly effective in suppressing HAZ-sensitization during subsequent gas tungsten arc welding. Laser surface treated HAZ of gas tungsten arc weldment exhibited significantly lower degree of sensitization and susceptibility to IGC than those of untreated HAZ. The degree of sensitization of untreated and laser surface treated HAZ specimens, as determined by double-loop electro-chemical potentio-kinetic reactivation (DL-EPR) test, are summarized in Table L.4.1. Enclosed figure (see Fig. L.8.1) compares untreated HAZ (marked as "N-HAZ") and pre-weld laser treated HAZ (marked as "LSM-HAZ") specimens of high carbon variety of stainless steel after undergoing IGC test, as per ASTM A262 practice E. It can be noticed from this figure that IGC tested untreated HAZ specimen broke into two pieces whereas pre-weld laser surface treated HAZ specimen remained uncracked.